

# We are IntechOpen, the world's leading publisher of Open Access books Built by scientists, for scientists

4,800

Open access books available

122,000

International authors and editors

135M

Downloads

Our authors are among the

154

Countries delivered to

TOP 1%

most cited scientists

12.2%

Contributors from top 500 universities



WEB OF SCIENCE™

Selection of our books indexed in the Book Citation Index  
in Web of Science™ Core Collection (BKCI)

Interested in publishing with us?  
Contact [book.department@intechopen.com](mailto:book.department@intechopen.com)

Numbers displayed above are based on latest data collected.  
For more information visit [www.intechopen.com](http://www.intechopen.com)



# Air Movement Within Enclosed Road-Objects with Contra-Traffica CFD-Investigation

M. Muhasilovic<sup>1,2</sup>, A. Mededovic<sup>1</sup>,  
E. Gacanin<sup>1</sup>, K. Ciahotny<sup>3</sup> and V. Koza<sup>3</sup>

<sup>1</sup>IPSA-Institute Sarajevo, Sarajevo

<sup>2</sup>The CIM-Collaboration Program of the GiZ  
German International Technology Agency

<sup>3</sup>The VSCHT – Institute for Chemical Technology, Prague

<sup>1</sup>Bosnia and Herzegovina

<sup>2</sup>Germany

<sup>3</sup>Czech Republic

## 1. Introduction

Accidents in closed-space traffic object do force for further investigation of a flow phenomena – that might be a consequence of such large-scale events. Benefit that almost directly would be coming out of this investigative approach is an optimal method for artificial ventilation, that must find mirroring in a annual statistics on covered roads[1, 2].

For such an investigative task, Computational Fluid Dynamics, the CFD offers ever stronger growing engineering tool. Once[3] passing through it's first sophisticated developments[4], the zone-model approach was not capable for solving the problems like those were treated by the field models for CFD-research. Generally, field-models are based on the full solution of the fundamental physical laws of energy-conservation, where the computational domain of explored large-scale phenomenon is divided in thousands of smaller control volumes; where mathematical mechanism after it's discretization are "translated" into programme-steps for computer handling. Today[5, 6], the CFD-society enjoys this software-development that started in 1960-ies and was certainly followed by the hardware development between mid '80-s and mid '90-s. Together, this computational mechanism [7-11] both hardware and software, can cope with computational domains with few thousands cells offering very satisfying results [1, 12] were accomplished attempts are done in both validating and exploring area of CFD. Modern field-model codes engaged in CFD-research, supported by today's powerful hardware, can cope with domains made out of several hundred thousands cells. Some computational codes[13] applied for tunnel-fires, are taking in account simple one-step chemistry for combustion modelling, and the reaction rate is won from a the eddy break-up mixing model[14]. This approach is suitable for turbulent diffusion flames as well – one of a characteristic of large-scale fires, where the rate of reaction is controlled by a mixing of fuel with oxidant (air). In such a step, solved would be (the time-averaged[15]), turbulence-modelled conservation-equations for mass, momentum, energy and species of combustion. The  $k-\varepsilon$  turbulence model with extra source terms accounting for the effect of

buoyancy in turbulent mixing would be applied in such numerical approach. Similar principle[2] in those sophisticated software, one can find[16] in the closed set of coupled equations that are again discretised and solved onto a three-dimensional finite-volume Cartesian mesh. In the latest phases of on-going software development several general purpose computer-programs for analysis of fluid flow - were developed[17] - that can handle both steady and transient flows. Anyhow, all of these research attempts (after their validation[18]), can document a good capability of the numerical approaches used in investigative treating both the reactive flows as well as large-scale fluid flow - especially in enclosed traffic objects.

## 2. Mathematical model

(In several reports, proceedings and papers, there was "no time" to mention the mathematic and numerical mechanism - due to the characteristic of those publishing media. Now, the opportunity here n will be used for the presentation of involved mathematic tool).

Applied explanation of the flow phenomena in the study[19] is explained by the Reynolds Averaged Navier-Stokes (RANS) equations, having turbulence treated by the k-ε model[20], representing the major characteristic of the applied CFD-investigation-tool of the FLUENT; and handling the buoyancy by applying the Boussinesq approximation. This approach, is not affected by fluctuation of initial conditions, offering more accurate presentation of the time dependent flow - particularly the distribution of the gaseous combustion products[21]. Since the investigations in the observed underground-space facilities have shown that the Mach Number was varying in the tolerance of the order between 0.003 and 0.022; such a flow can be presumed as incompressible[22]. So assumed as incompressible, the fluid while crossing the reaction front, doesn't undergo thermal-caused expansion and the reaction makes no impact onto flow-velocity. Further assumption, to have a planar propagation front of combustion in a motionless fluid, leads to the application of the Boussinesq approximation[23] without external forces[24]. Boussinesq buoyancy model is corresponding to the infinitely small difference of density between combusted fluid and fuel. Here, the flow velocity obeys the incompressible Navier-Stokes equation with a temperature-dependent force term[24]. The change of temperature  $0 \leq T \leq 1$  is described by an advection-reaction-diffusion equation. For this to-be-investigated incompressible gaseous reactive flow at low velocity, the governing equations of the combustion-induced flow read:

$$\frac{\partial \bar{v}_j}{\partial x_j} = 0 \quad (1)$$

$$\frac{\partial \bar{v}_i}{\partial t} + \frac{\partial (\bar{v}_i \bar{v}_j)}{\partial x_j} = -\frac{1}{\rho} \frac{\partial \bar{p}}{\partial x_i} + \frac{1}{\rho} \frac{\partial \bar{\tau}_{ij}}{\partial x_j} - g_i \alpha \Delta \bar{T} \quad (2)$$

$$\frac{\partial \bar{T}}{\partial t} + \frac{\partial (\bar{T} \bar{v}_j)}{\partial x_j} = \frac{\partial}{\partial x_j} \left( \frac{\lambda}{\rho c_p} \frac{\partial \bar{T}}{\partial x_j} \right) + \frac{1}{z} R(T) \quad (3)$$

Here, we recognise  $\bar{v}_i, \bar{v}_j$  as average velocity components,  $\bar{T}$  as averaged local temperature,  $\rho$  as density,  $t$  as time and  $x_i, x_j$  as space coordinates. The  $R(T) = \frac{1}{4} T (1 - T)$  stands for

reaction rate[24] where the reciprocal value of reaction time-scale is represented by  $1/T$  and  $\rho$  is here again a constant average density. Temperature  $T$  will be used as expression for reaction-progress-variable as well, whose purpose is to distinguished burned, unburned and partially burned state, providing facile interpretation of flame propagation. The term  $-g_i\alpha\Delta\bar{T}$  denotes buoyancy, treated according to the Boussinesq approximation, where  $\Delta\bar{T}$  is showing the difference between local and reference temperature. The symbol  $g$  denotes the gravity and  $\alpha$  is coefficient of the thermal linear deformation. The model for the unknown Reynolds stress[25],  $\partial\bar{\tau}_{ij,s}$  is related to the local strain rate:

$$\tau_{ij} = (\tau_{ij})_N + (\tau_{ij})_T \quad (4)$$

where we distinguish between Newtonian stress  $(\tau_{ij})_N = 2\mu\bar{S}_{ij}$  featuring molecular viscosity; and turbulent Reynolds stress  $(\tau_{ij})_T = 2\mu_T\bar{S}_{ij}$  featuring turbulent viscosity recognising again  $\bar{S}_{ij}$  as local strain stress rate reads:

$$\bar{S}_{ij} \equiv \frac{1}{2} \left( \frac{\partial v_i}{\partial x_j} + \frac{\partial v_j}{\partial x_i} \right) \quad (5)$$

Here we recognise the turbulent viscosity:  $\mu_T = C_\mu \frac{k^2}{\varepsilon}$  (6)

The applied k- $\varepsilon$  model[26] is a two-equation eddy viscosity model [27, 28] uses transport equations for these two variables[29]. One of these equations governs the distribution through the field of  $k$ , the local kinetic energy of the fluctuating motion. The other one is explaining a turbulence characteristic of different dimensions, the energy dissipation rate  $\varepsilon$  [30].

$$\frac{\partial k}{\partial t} - \nabla \cdot \left( C_\mu \frac{k^2}{\varepsilon} \nabla k \right) = C_\mu \frac{k^2}{\varepsilon} P_d - \varepsilon - \lambda_v N^2 \quad (7)$$

$$\frac{\partial \varepsilon}{\partial t} - \nabla \cdot \left( C_\varepsilon \frac{k^2}{\varepsilon} \nabla \varepsilon \right) = C_1 k P_d - \frac{\varepsilon}{k} (C_3 \lambda_v N^2 + C_2 \varepsilon) \quad (8)$$

The  $P_d$ , the production term for the squared shear frequency is:

$$P_d = \frac{1}{2} \left( \left\| \nabla V + \nabla V^T \right\| \right)^2 \quad (9)$$

where  $\left\| \nabla V + \nabla V^T \right\|$  is the 2-norm matrix. The constants are given:  $C_1 = 0.126$ ,  $C_2 = 1.92$ ,  $C_\mu = 0.09$ ,  $C_\varepsilon = 0.07$ . The variable  $N$  denotes the Brunt-Väisälä frequency, with the  $N^2$ , related following squared buoyancy:

$$N^2 = -\frac{v_v}{\sigma_t} \frac{g}{\rho_0} \frac{\partial \rho}{\partial z} \quad (10)$$

Here is constant  $\sigma_t = 1$  and following expressions of eddy coefficients  $v_v$ ,  $\lambda_v$  should include the stability parameters to account for the turbulence damping in the stratified fluid flows:

$$v_v = S_u \frac{k^2}{\varepsilon} + v, \quad \lambda_v = S_b \frac{k^2}{\varepsilon} + \lambda_b \quad (11)$$

$$S_u = \frac{0.108 + 0.0229\alpha_N}{1 + 0.47\alpha_N + 0.0275\alpha_N}, \quad S_b = \frac{0.177}{1 + 0.043\alpha_N} \quad (12)$$

where  $\lambda_b = 10^{-6}$  and the following stability coefficients  $\alpha_N$  and  $C_3$  can be expressed as:

$$\begin{aligned} \alpha_N &= \frac{k^2}{\varepsilon^2} N^2 \\ C_3 &= -0.4; N^2 > 0 \\ C_3 &= 1; N^2 < 0 \end{aligned} \quad (13)$$

During these investigations, the wall shear stress was obtained from the logarithmic law of wall ("wall function") for the distance from the wall,  $y$ , the von Karman constant  $\kappa=0,41$  and the constant  $C=9,793$ :

$$\frac{\bar{v}}{v_\tau} = \frac{1}{\kappa} \ln C \frac{v_\tau y}{v} \quad (14)$$

Energy transfer within the computational domain of such non-premixed turbulent flow in tunnel cavity is governed by next equation:

$$\frac{\partial H}{\partial t} + \nabla \cdot (\bar{v}H) = \nabla \cdot \left( \frac{\gamma_t}{c_p} \nabla H \right) + Q_h \quad (15)$$

where contribution to the energy budget, characterised through turbulent thermal conductivity  $\gamma_t$  is performed through the heat conduction and diffusion combined in term  $\nabla \cdot \left( \frac{\gamma_t}{c_p} \nabla H \right)$ , accompanied by the heat-increase component  $Q_h$  due to the chemical reaction rate  $R$  of a species  $n$  and it's molar mass  $M$ :

$$Q_h = - \sum_n \frac{h_n^0}{M_n} R_n \quad (16)$$

In the governing energy equation is total enthalpy  $H$  based onto particular enthalpy of the  $n^{\text{th}}$  species  $H_n$  and it's mass fraction  $Y_n$

$$H = \sum_n Y_n H_n \quad (17)$$

with

$$H_n = h_n + h_n^0 \quad (18)$$

having so species  $n$  characterised through it's thermal capacity  $c_{p,n}$  and  $n^{\text{th}}$  enthalpy  $h_n = \int_{T_{ref}}^T c_{p,n} dT$  with referent temperature  $T_{ref} = 293,15K$  that makes an impact on the formation enthalpy  $h_n^0(T_{ref,n})$ .

The radiative transfer equation (RTE) for an absorbing, emitting and scattering medium at the position  $\vec{r}$  in the direction  $\vec{s}$  reads:

$$\frac{dI(\vec{r}, \vec{s})}{ds} + (a + \sigma_s)I(\vec{r}, \vec{s}) = ax^2 \frac{\sigma T^4}{\pi} + \frac{\sigma_s}{4\pi} \int_0^{4\pi} I(\vec{r}, \vec{s}')\Phi(\vec{s}, \vec{s}')d\Omega' \quad (19)$$

The applied Discrete Ordinate approach for treating the radiation considers the RTE in the direction  $\vec{s}$  as a field equation, allowing the modelling of non-gray radiation, using the gray-band model. So, for the spectral intensity  $I_\lambda(\vec{r}, \vec{s})$  the RTE can be written as:

$$\nabla \cdot (I_\lambda(\vec{r}, \vec{s})\vec{s}) + (a_\lambda + \sigma_s)I_\lambda(\vec{r}, \vec{s}) = a_\lambda x^2 I_{b\lambda} + \frac{\sigma_s}{4\pi} \int_0^{4\pi} I_\lambda(\vec{r}, \vec{s}')\Phi(\vec{s}, \vec{s}')d\Omega' \quad (20)$$

Here is  $\vec{r}$  a position vector and  $\vec{s}$  a direction vector.  $I$  denotes the radiation intensity, i.e. radiation intensity  $I_\lambda$  for a certain wave-length  $\lambda$ . The radiation intensity for the black body reads  $I_{b\lambda}$ . Scattering coefficient is represented by  $\sigma_s$  and Stefan-Bolzman-constant reads  $\sigma = 5.672 \times 10^{-8} \text{W/m}^2\text{K}^4$ .  $\Phi$  stands for phase function,  $T$  is local temperature and  $x$  is refractive index. Path length is  $s$  and  $\vec{s}'$  denotes direction vector.  $\Omega'$  stands for solid angle and  $a$  is absorption coefficient, i.e. absorption coefficient for a particular wave-length  $a_\lambda$ . So will the RTE be integrated over each wave-length-interval  $\lambda$  resulting in transport equation for entity  $I_\lambda \Delta\lambda$ , containing the radiant energy of the wave-length  $\Delta\lambda$ . The total intensity  $I(\vec{r}, \vec{s})$  in each direction  $\vec{s}$  at some position  $\vec{r}$  is computed as:

$$I(\vec{r}, \vec{s}) = \sum_n I_{\lambda,n}(\vec{r}, \vec{s})\Delta\lambda_n \quad (21)$$

The weighted-sum-of grey-gases model (WSGGM), that was applied in this study for handling the irradiance in the complicated phenomenon of the confined combustion[31] presents a reasonable compromise between the oversimplified grey gas model and a complete model which takes into account particular absorption bands. Within the Discrete Ordinate approach, where the soot generation[32] was described by the Magnussen model[28], the basic assumption of the WSGGM means that the emissivity  $E$  of the any  $n^{\text{th}}$  gray gas characterised by  $p_{\text{SUM}}$ , the sum of it's partial pressures  $p$  and the absorption  $\kappa$  within the computational domain over a distance  $d$  is presented by:

$$E = \sum_{n=0}^i a_{E,n}(T) \left(1 - e^{-\kappa_n p_{\text{SUM}} d}\right) \quad (22)$$

Here  $a_{E,n}$  denotes the emissivity weighting factor for the  $n^{\text{th}}$  gray gas and  $(1 - e^{-\kappa_n p d})$  is emissivity of the  $n^{\text{th}}$  gray gas. The temperature dependence of  $a_{E,n}$  is commonly

approximated by the relation: 
$$a_{E,n} = \sum_{n=1}^J b_{E,n} T^{n-1} \quad (23)$$

where polynomial coefficient  $b_{E,n}$ , depending on the gas temperature emissivity is obtained experimentally. The coefficients  $b_{E,n}$  and  $\kappa_n$  are slowly changing for broad range of the

pressure ( $0.001\text{bar} \leq p \leq 10\text{bar}$ ) and temperature ( $600\text{K} \leq T \leq 2400\text{K}$ ) which simplifies

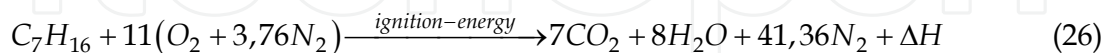
relation (22) to:

$$E = \sum_{n=1}^J a_{E,n} \kappa_n p_{SUM} \quad (24)$$

for

$$a = \sum_{n=1}^J a_{E,n} \kappa_n p \quad ; \quad s \leq 10^{-4} \text{m} \quad \text{and} \quad a = -\frac{\ln(1-E)}{s} \quad ; \quad s \geq 10^{-4} \text{m} \quad (25)$$

The combustion - the chemistry development is explained by fast chemistry assumption including the prePDF [33] and in the ideal stoichiometric conditions the reaction runs as follows:



However, in a case of unfulfilled combustion, soot is influencing the radiation absorption. Employed generalised model estimates the effect of the soot onto the radiative heat transfer by determining an effective absorption coefficient for soot. In this case, absorption coefficient is a sum of the one for the pure gas  $a_g$  and that one for the pure soot  $a_s$  :

$$a_{s+g} = a_s + a_g \quad (27)$$

The  $a_g$  is obtained from presented WSGGM approach and

$$a_s = b_1 \rho_m [1 + b_T (T - 2000)] \quad (28)$$

with  $b_1 = 1232,4 \text{ m}^2/\text{kg}$  and  $b_T \cong 4,8 \cdot 10^{-4} \text{ 1/K}$ , where  $\rho_m$  denotes soot density.

### 3. Numerical approach

Discretizing the governing equations in both space and time [28, 34] while choosing the numerical method of the standard finite volumes [22, 34, 35], the CFD-tool is "adapted" for the time-dependent modelling of the explored event. The spatial discretization of time-dependent equations within here-employed segregated solution method are linearized in an implicit way. Since variables described the flow by their value at the centre of a single mesh-cell in explored computational domain, the system of linear equations occurs, containing mentioned unknown variable at the cell centre as well as their unknown values in neighbour cells. A scalar transport-equation within such method is also used to discretize the momentum equations; in the same mode for the pressure-field (if cell-face mass-fluxes were known). This applies for velocity-field as well. In case that the pressure-field and face mass fluxes are not known, applied commercial software of *FLUENT* [28] uses a co-located scheme, whereby the local values for pressure and velocity are stored at centres of a single mesh-cell. A need for interfacial values includes an application of an interpolation scheme to compute pressure and velocity out of mesh-cell values. The integration over the observed control-volume, where is a mesh-cell in a computational domain, can be performed yielding the discretised equation for the mass-flux through a control-surface - a mesh-face on the mentioned mesh-volume. Procedure of the segregated solver that follows as a mechanism in this research, the continuity equation, is used as an equation for pressure as well [28].

However, the pressure does not appear for an incompressible flow in explicit way, since the density is not directly related to pressure. However, through the application of the *SIMPLE*-algorithm-family[34] during this investigation (within the commercial software package of *FLUENT*) the won values for pressure were introduced into the continuity equation and in this way supported the pressure-velocity coupling. This was done through the *NITA*-algorithm for the unsteady.. Further, the *SIMPLE* uses a relationship between velocity and pressure corrections to enforce mass conservation and to obtain the pressure field. So, executing these numerical steps, the equations can express the state for each other cell in the computational grid, the mesh. This will result in a set of algebraic equations with a coefficient-matrix. In this way the segregated solver is “updating” variable-field by considering all the cells of the domain in the same time, solving the governing equations sequentially (segregated one from another). What follows are the iterations of the solution-loop before one wins the converged solution. Subsequently, the next field of another variable will be solved by again considering entire cells at the same time, etc. Finally, determining of the boundary conditions relied on some previous done studies [19, 36] that were basis for the estimation.

#### 4. Objects of investigation - Two different tunnel-shapes

Today’s major two shapes of the underground traffic (road) facilities that are having their cross-section as a “horse-shoe” and rectangular shape – we explored here. And according to the final use, these traffic covered object, were taken as very frequently used ones. Additionally, those tunnels (one, having bifurcation – is going under Slovenian Capital of Ljubljana, and another is situated in a curvy valley of the river Bosna, between Bosnian cities of Travnik and Zenica) are “offering” interesting geometry for a CFD-based investigation; such is air-movement and the movements of air-pollutants and other gaseous products (in accidental situations).

##### 4.1 The “Sentvid” tunnel

As mentioned, the northern tube of tunnel “Sentvid” (undergoing the city of Ljubljana) was investigated with the CFD-approach, where the “chimney-effect” was expected (coming from bifurcated part of the elevating trek, which comes out, up to the city-streets) Although well performed acquisition of data during the 3,5MW-fire-experiment, Slovenian Road Administration (DARS) was not able and/or allowed to organize the test for longitudinal ventilation in case of 40MW-fire event. In this scenario, during it’s functioning, the artificial ventilation should response by the 2<sup>nd</sup> minute, securing so the area of accident, by suppressing the temperatures that can provoke concrete-destruction. Therefore, a CFD-based approach towards this important question was here an optimal choice. Particularly because of the fact that the “Sentvid” tunnel is having a change from it’s rectangular cross-section’s shape (in it’s old part) into it’s new part that has “horse-shoe” shape of the cross-section (when one is “rising” from it’s western exit to Ljubljana). Further characteristic of this investigated north-tube is that the western exit (towards city of Kranj) is lying geodetically lower then it’s Entrance from Ljubljana. So is the natural air-flow always confronted with the traffic-flow which is always against it.

Going about 50m in the north tube away from the interchange between the old-part of the “Sentvid” towards it’s new (“horse-shoe”-shaped) part – the presumed accidental fire-place



is situated. In order to produce thermal load of 40MW heat release, from the surface that corresponds to the dimensions of the used pan in the experiment (1m x 2m) the mass flux of the inflammable agent (the heptane) was set to 0.889kg/s (as same as during the CFD-based investigation of the artificial accidental fire-case).

The northern tube of "Sentvid", with the slope of 2,2 %, has two major main-curves with a Radius of 4000m and 1500m, where the "horse-shoe" cross-section determines the first 1080m of the tunnel. Starting as a three-lane tunnel, after the bifurcation (on the 720<sup>th</sup> meter of its length, going from Ljubljana-entrance) the "main stream" of the tunnel "continues" as a two-lane traffic communication towards Kranj-exit; and the bifurcated "horse-shoe-shaped" tunnel-line elevates and exits to the point of about 12m above the road-level of the main tunnel-stream, with the length of a further 400m and a change from an one-lane to the two-lane "horse-shoe" cross-section. Therefore, the Aspect-Ratio changed in this tunnel: for three-lanes part  $Ap = 1,707$  to the rectangular and other horse-shoe-shaped part with two lanes with  $Ap = 1,32$ . Tunnel-entrance as open (pressure) boundary was used for initializing computational values for the velocity and pressure in the computational-domain since the global temperature was set to the 300K. The tunnel housing, tunnel road and tunnel walls, were presumed to be heat transparent.

#### 4.2 The "Vranduk" tunnel

Another tunnel which was object of interest and it is in a well active use in the road-network through the Highlands of Bosnia and Herzegovina - is a motorway-tunnel of "Vranduk-2" that is binding two Bosnian cities of Travnik and Zenica. "Vranduk-2" was chosen because of the it's geometry, made in the road-curve of radius of  $r=1000m$  after about 80m straight road through it, where it's cross-section, in a shape of a "horse-shoe", has an almost constant aspect ratio of ( $As=1.49$ ). In it's length of 1067m, the explored tube of "Vranduk-2" has a denivelation between geodetically higher, eastern entrance from Zenica-side downwards to exit at the Travnik-side of 8.37m. For this CFD-based investigation, the tunnel-entrance and -exit were characterised as open (pressure) boundaries. The drop i.e. increase of 1.48Pa at the entrance and tunnel-exit, respectively, as well as overall air-movement of 1.1m/s were used for initializing the values in computational domain for the velocity and pressure, since the global temperature was set to the 300K. The fuel "pool" - the simulated fire-place, has been determined by the constant max flux rate of 0,889kg/m<sup>2</sup>s[37] having hydraulic diameter of 1,333m for a 40MW-heptane fire[38]. The tunnel housing, tunnel road and tunnel walls as well, were presumed to be heat-transparent fences of the investigated "Vranduk-2" tunnel-tube; and this especially - because of the-type of the soil, where tunnel situated[39]. This decision was based on so-far research-experience, but also on the reality-oriented investigation on modern tunnel-construction, that obeys the thermal conductivity of a rock where through a tunnel would be built. Particularly for the "Vranduk-2" tunnel, that was built in the carstic area, in the Bosnian Highlands, the specific thermal conductivity of such rocks ( $\lambda = 2,3W/mK$ )[39, 54].

#### 4.3 Computational domain

The area in which the computation with applied mathematical model and subsequent performed numerical discretization, was the very volume, that can take a fluid (an air, or in case of accidental fire, the combustion gaseous products) i.e. the housing of the tunnel.

Therefore there are two computational domains to be distinguished: the “Sentvid” underground highway-facility that undergoes the Slovenian Capital of Ljubljana; and the “Vranduk-2” tunnel-tube - both of them as the traffic communications, very frequently used.

#### 4.3.1 The Slovenian tunnel

While meshing the Slovenian tunnel, two kinds of grids (having two kind of characteristic basic cells) were applied. So, in the area of the domain where the major fluid-mechanic and thermodynamic occurrences are expected, the unstructured tetrahedral mesh was installed. In this part, where the pool with the mentioned fuel flux rate of 0,899kg/s is situated and the pool-surface temperature is 500K, a combined asymmetric mesh was employed. This mesh has different density, having characteristic cell size of 60mm up to 200mm from one side of the middle-plane of the Tunnel. Such approach was about to approve that the gained solution is mesh-independent. The other parts of the 1470m-long tunnel with alternating surface of the cross-section is meshed with unstructured penta-hedral mesh, following the explained general image of the asymmetric mesh. The entire computational domain is meshed with round 4.400.000 cells.

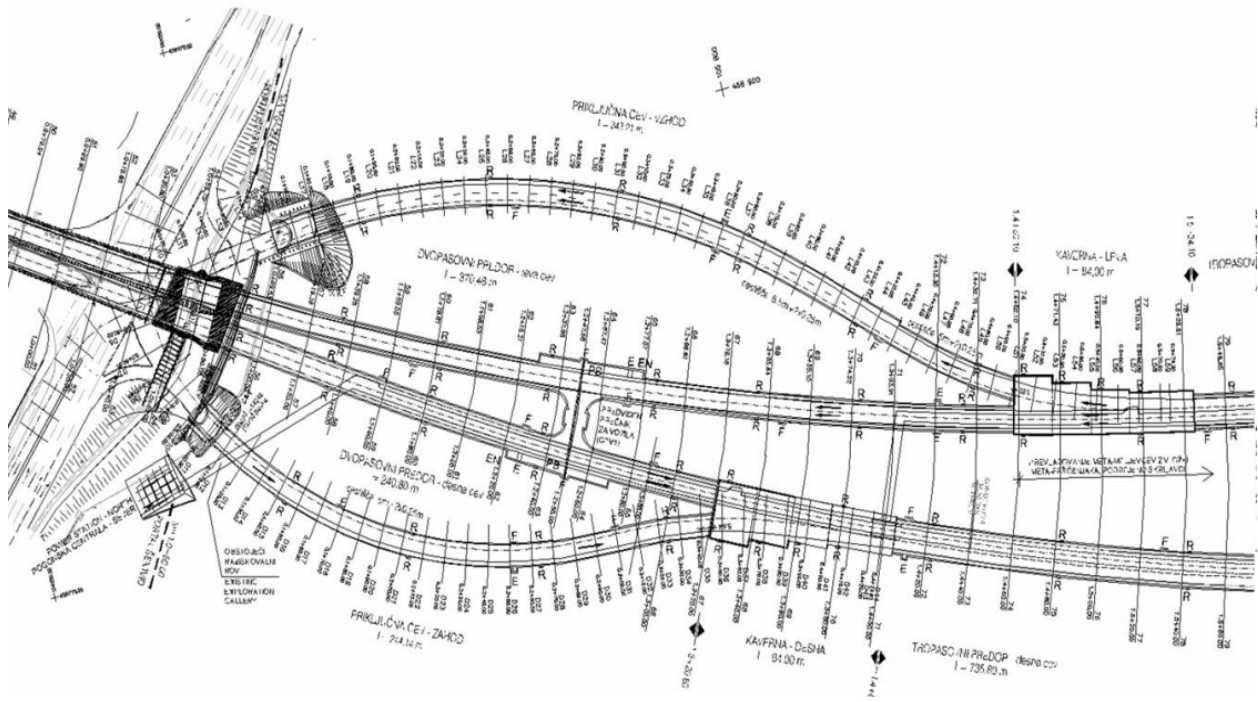


Fig. 4.2.1-1. Both north and south tube of the Sentvid tunnel

As mentioned, the tunnel-housing as well as the tunnel-road in the computational domain were defined as heat-transparent walls and fluid-domain is air with the ambient conditions and no movement. The entrance as well as the tunnel-exit, are defined as open-pressure boundaries. All of these facts were used for the initialisation.

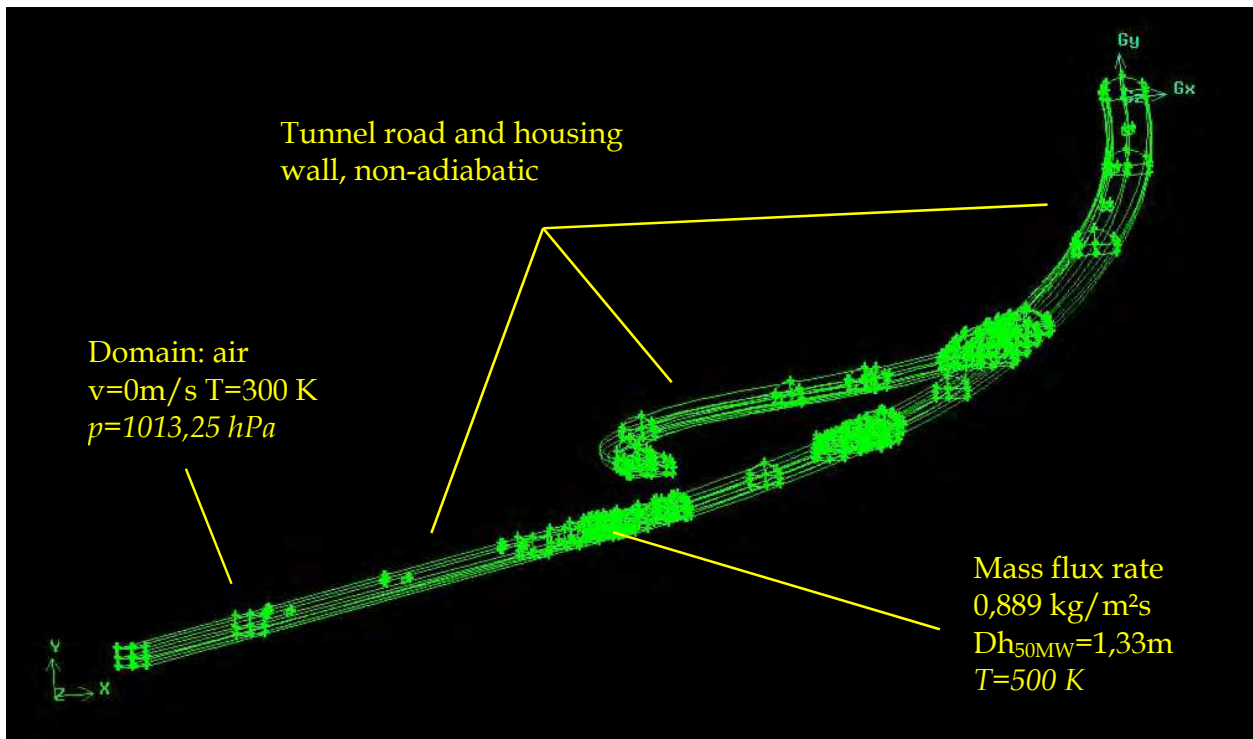


Fig. 4.2.1-2. North tube of the “Stentvid” tunnel in computational domain

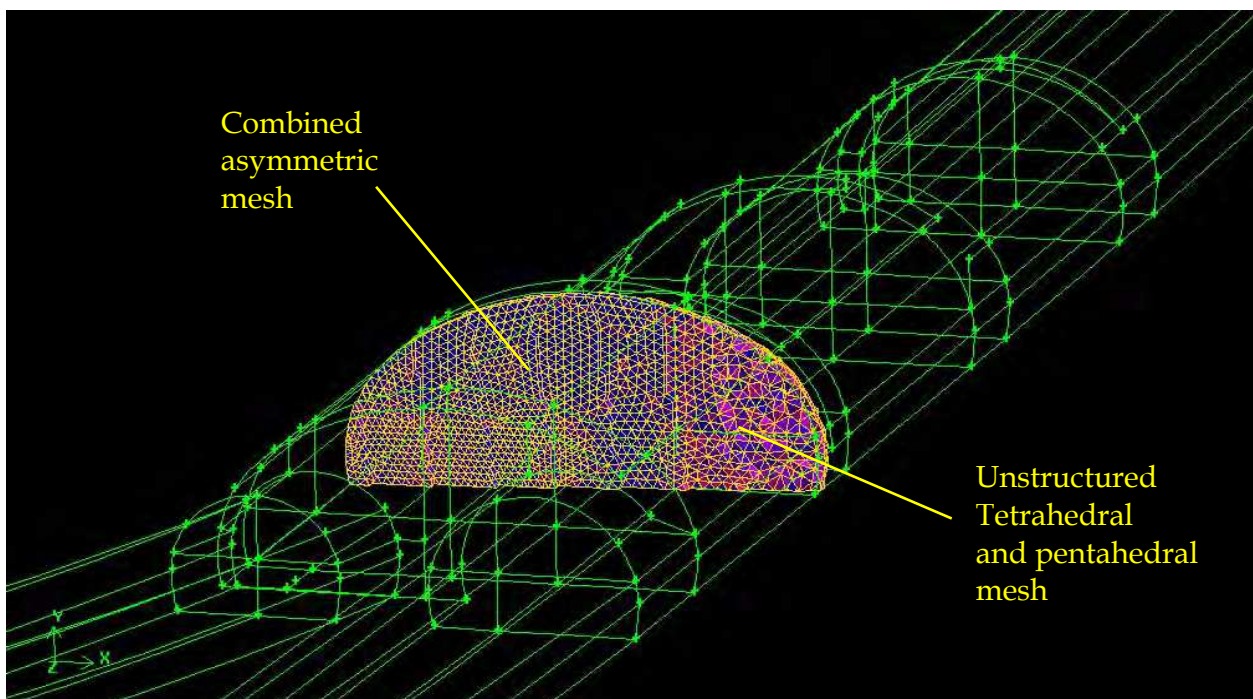


Fig. 4.2.1-3. Meshing – the near-bifurcation zone

### 4.3.2 The Bosnian tunnel

The mesh of this computational domain is also determined by tetrahedral-, pentahedral- and hexahedral-cells of a random structure. In this case a denser grid was also applied in the area around the fire-pool, having so more grid-points to support the major fluid-mechanic and thermodynamic occurrences. Such unstructured mesh was installed in whole computational domain. However, the subsequent parts of the 1067m long tunnel with non-alternating cross-section, are also meshed with unstructured pentahedral and hexahedral cells in the explained way, having increased cells sizes from 400mm up to 800mm – as one gains on distance from fire pool, towards the tunnel-exit and entrance. The pool with the fuel had a flux-rate of 0,899kg/s as well, and the pool-surface temperature is set also to 500K. Middle-plane of the Tunnel was going throughout the domain following the curvature of this cavity.

The tunnel-housing and the tunnel-road were in the computational domain defined as non-adiabatic walls as well; and fluid-domain is air, with the ambient conditions and fluid-movement of 1,1m/s as natural draft. The entrance from the side of the city of Zenica as well as the tunnel-exit at the Travnik-side, are in this case also defined as open-pressure boundaries with the mentioned pressure-decrease i.e. pressure surplus of 1.48Pa.

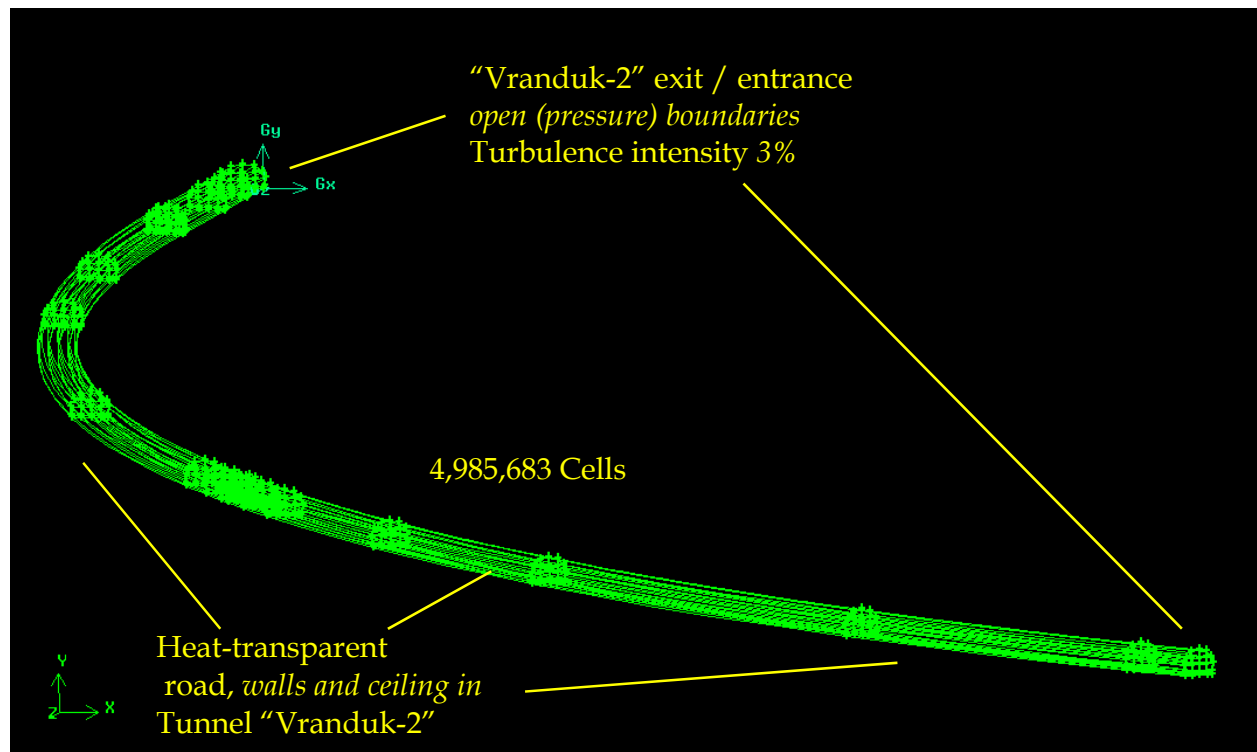


Fig. 4.2.2-1. The computational domain "Vranduk-2"

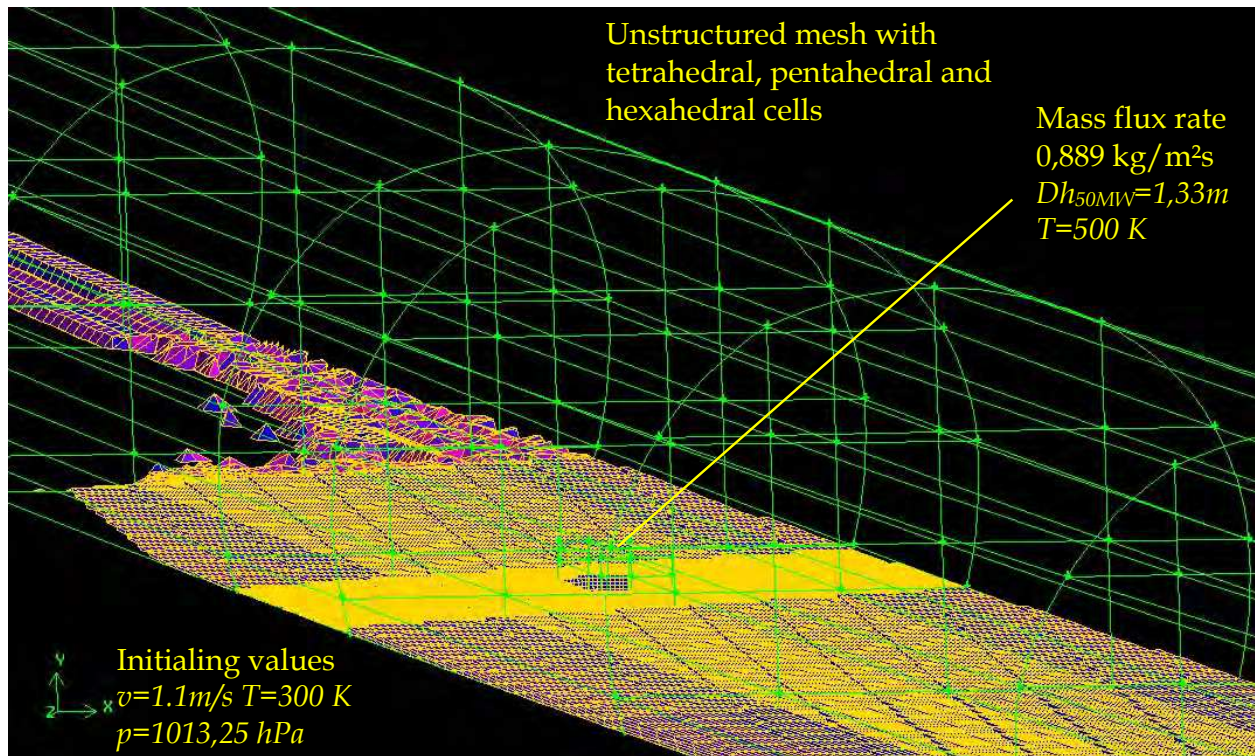


Fig. 4.2.2-2. The unstructured mesh in "Vranduk-2", at one fourth of it's length

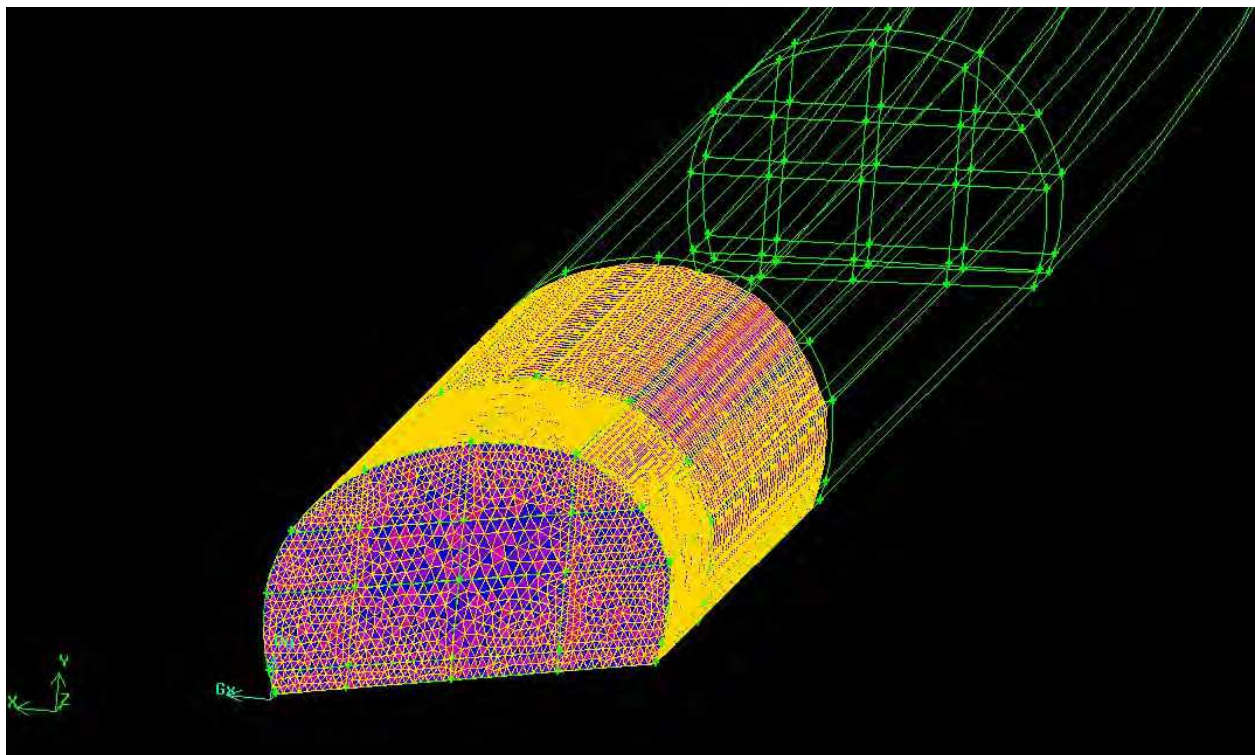


Fig. 4.2.2-3. "Vranduk-2"-exit towards city of Zenica meshed randomly - pentahedral cells

## 5. Discussion of the observed phenomena – Bosnian tunnel

Although applied onto the scaled model in physical experiment, a well defining the phenomena of the confined accidental thermal load (while flame was impinging up to the tunnel-ceiling), was introduced by Kurioka et. al.[41] as well as the additional characteristic phenomenon of the “rolling”, when fire in enclosure[41] is “leaving” the original combustion-place. In this light it is to distinguish two major groups of the flame-shapes in enclosure: the ones, that impinge on the tunnel roof and the others that, influenced by the longitudinal air-stream, that do not. During the CFD-investigations of the large-scale flow phenomena, in both of the tunnels, one could recognise obviously the first ones, where such art of the large-scale flame could be cause for stronger damage on the Reinforced Concrete tunnel-construction.

### 5.1 The “Sentvid” highway-tunnel

The unwanted effect of the large-scale accidental fire can be noticed during the numerical experiment in the north tube of “Sentvid”, where in first simulated scenario, the employment of the longitudinal ventilation set was not foreseen. This built-in system should react by the 2<sup>nd</sup> minute of such accidental thermal load, where until then the Reinforced-Concrete-Construction of a tunnel ought to withstand the thermal load.

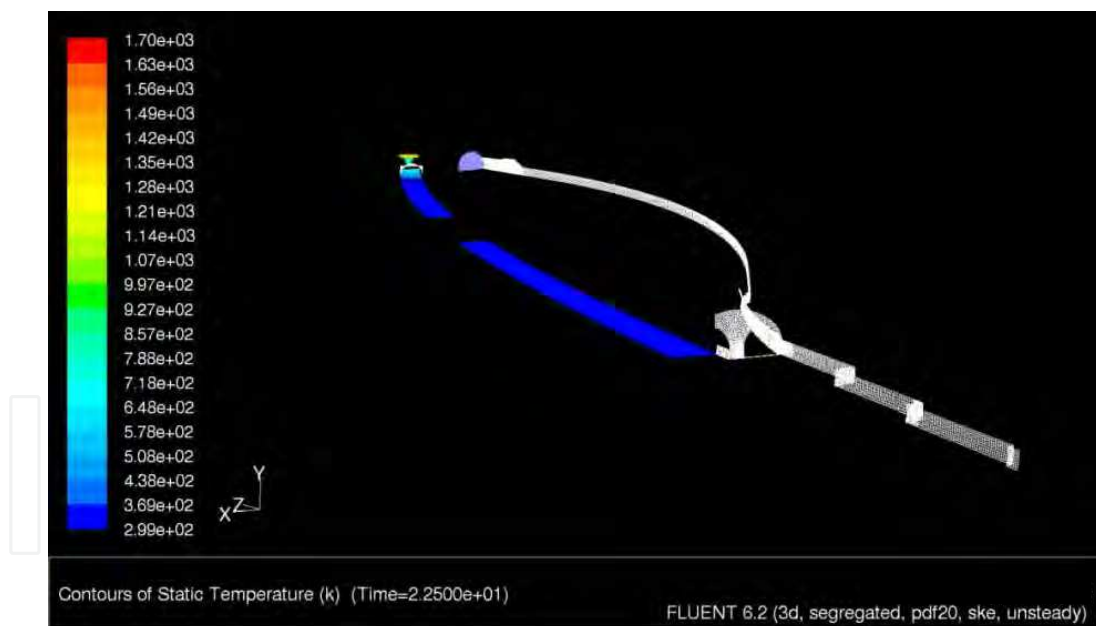


Fig. 5.1-1. A view to a part of the computational domain for the north tube of the “Sentvid”-highway-tunnel. In right part of the sketch, “coming” from the East, one can notice the begin of the bifurcation zone, marked through the part of the grid, after which highway-exit-trek is rising right up to the surface and left part is “continuing” towards the West. At the very end of this highway-section, in this part of computational domain, the modelled fire-place was set. The artificial ventilation was not employed yet.

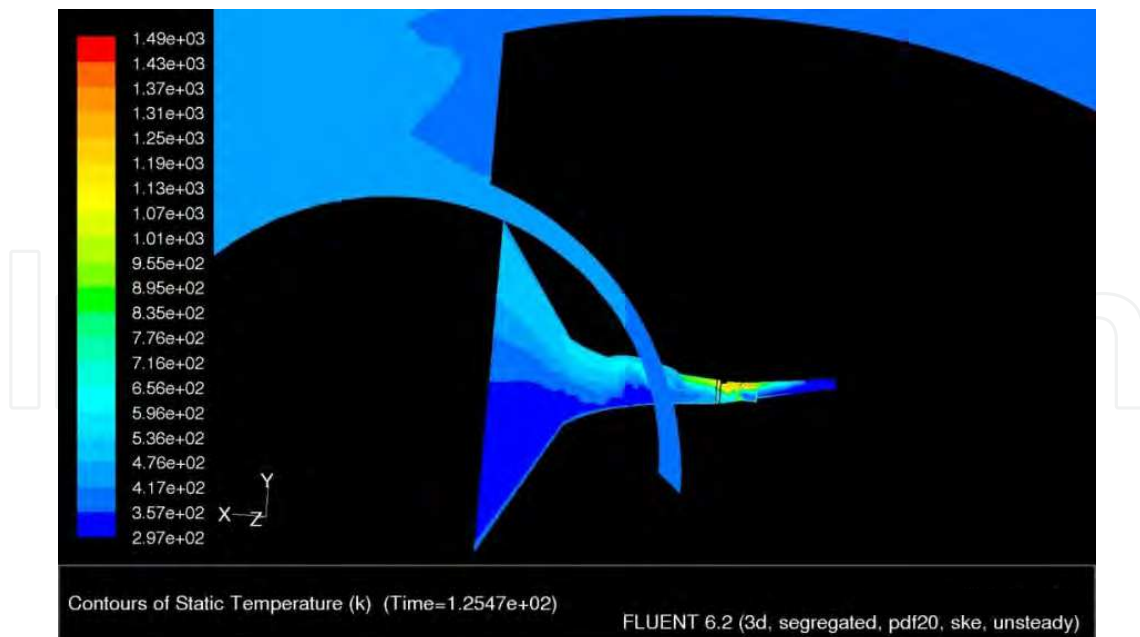


Fig. 5.1-2. “Standing” in the bifurcation zone of the north tube in “Sentvid”. After the 2<sup>nd</sup> minute, the spreading of the volatile combustion products is not confronting with longitudinal ventilation and it is rising towards the higher geodetic position at the eastern tunnel-entrance is established, while the fire-place (in the bottom of this CFD-recorded moment) is forcing the hot gases to reach the western tunnel-exit.

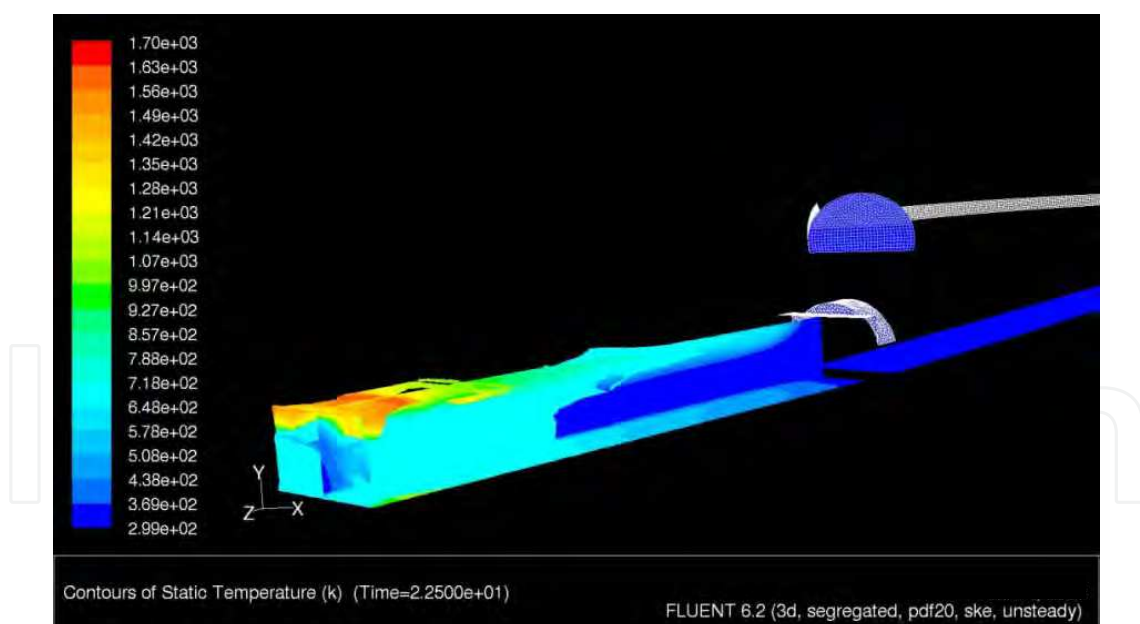


Fig. 5.1-3. Observed computational domain in the north tube of the “Sentvid-highway-tunnel: On the iso-surfaces that present draft-velocity of 4m/s due to the ventilation towards western exit, as well as on the central plane, the back-layering phenomenon is to be noticed. Since the flow of the ventilated air is still not entirely established, the movement of the hot gaseous products in 22<sup>nd</sup> second of accidental combustion is reaching the interchange between old and new tunnel-part - here made recognizable by the mesh-display of this tunnel-part (and just above it - although totally separated - is highway-tunnel-exit to the “surface”).

Having firstly no artificial ventilation, the surroundings in northern cavern of the “Sentvid”-tunnel in first 22s during the numerically performed investigation (with applied  $k-\epsilon$  turbulence model) supported the expected phenomenon of natural buoyancy towards the higher geodetic position. However, the set draft into the computational domain, caused by mentioned artificial ventilation (and according to the real-case scenario, due to the traffic-flow in opposite direction) is providing that the axis of the flame is pushed away, down the tunnel-“slope”. This is because of the relative weak buoyancy, compared to the mentioned forced longitudinal air-movement[41]. As one moves further of the fire-source, towards the western tunnel-exit, the buoyancy gains on the strength due to the increased temperature, as we observe an impinging of the flame.

The aim of the to-be-employed ventilation in such accidental event is not to contribute to the extinguishing, but to limit the unwanted thermal load of a 40MW-fire and to conquer the distribution of hot gaseous products and their negative impact. This urged occurrence can be noticed in record of the 88<sup>th</sup> second of numerical modelling on establishment of the accidental fire and propagation of it’s consequences (Figure 5.1-4), where one can notice additional agreement with the approaches in some physical simulations[42,46] as well. So, the flame and/or hot gas-current do not impinge on the tunnel ceiling, but (enveloped by the ventilation stream) are heading towards “Sentvid’s” western (and geodetically lower) exit. The stream of the hot gases is losing the temperature through the convection-mechanism, the buoyant effect is becoming weaker and the damaging of the Reinforced-Concrete-Construction is limited. Although still present, back-layering along the ceiling is falling down since the gaseous combustion products are being mixed with the cooler fan-air (Fig. 5.1-4) However, the tunnel road remains under the unwanted impact of the thermal load.

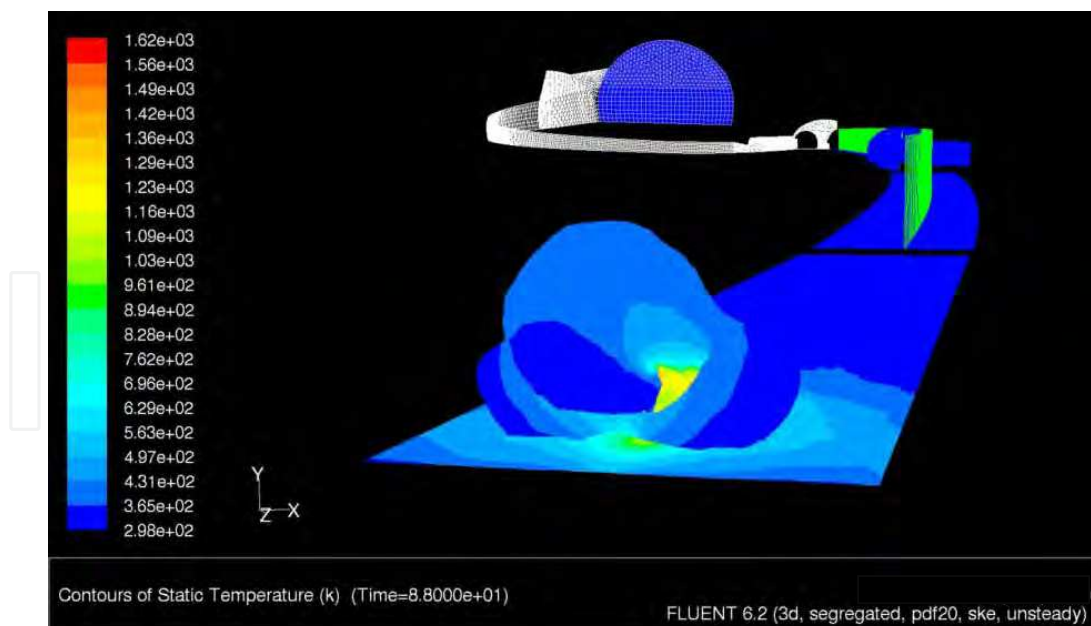


Fig. 5.1-4. The CFD-record of the 88<sup>th</sup> second: on the iso-surfaces of the 4m/s-velocity-magnitude, displayed temperatures coming from the accidental fire-event are not to pose any threat to the RC-construction of the tunnel. The thermal energy, demonstrated to the surroundings by the convection and irradiance, is being transferred. However, the accidental thermal load is further-on negatively influencing the material of tunnel-road.



Additional size of the impact of longitudinal artificial ventilation offers a view of the fire-place (Fig 5.1-5) in the 120<sup>th</sup> second of this accidental-event. In this large-scale reactive flow – the mixing processes and the chemical reactions with their physical consequences are more expressed. So, on the central plane (that intersects the fire) with the established temperature-fields, one can notice the “hotspots”, occurred, due to the fluctuations in the combustion. This is to be understood as a constructive interference of the buoyancy with the longitudinal flow (towards the western lower geodetic position) - wherever the buoyant forces are stronger than convection of the fire plume and hot gas-stream, which is in the near-fire-area. These occurrences do present in this phase of the fire-development already a dangerous point for the construction of the tunnel body (Fig. 5.1-5). Further observation of the temperature-impact is holding however no proof for interaction between the cavern-curvature and the distribution of the large-scale fire consequences (Fig. 5.1-3, -4, -5) and combined plots of the temperature with velocity iso-surfaces did not point up to expected “chimney effect” due to the tunnel’s bifurcation and tube of the exit-trek. In it’s 120<sup>th</sup> second, the employed longitudinal ventilation has appear as successful enveloping of the large-scale-fire event and it’s negative consequences throughout the “Sentvid’s” north-cavern.

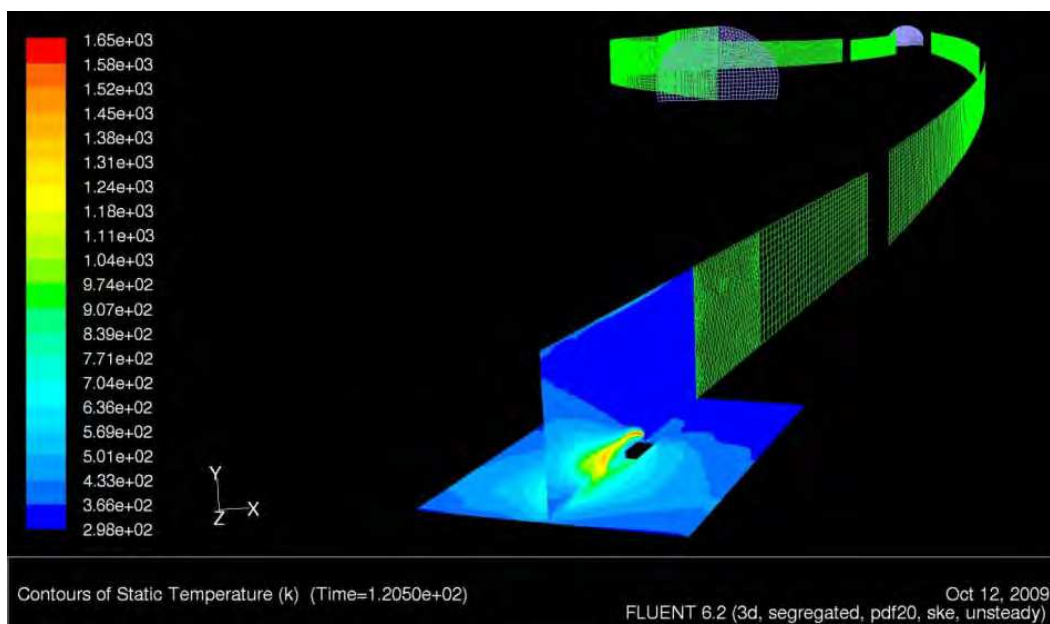


Fig. 5.1-5. The CFD-record of the 120<sup>th</sup> second: on the central plane that goes through the fire, displayed temperatures coming from the accidental-event are not to pose any threat to the RC-construction of the tunnel, since the fire-event is fully enveloped by the ventilated air-stream. The thermal energy, demonstrated to the surroundings, is being transferred into the air-flow. However, the accidental thermal load is further negatively influencing the material of the tunnel-road (here: a view towards the eastern entrance: far in the sketch in bifurcation zone. Above the fire-place, we see the tunnel exit)

## 5.2 The “Vranduk-2” road-tunnel

Situation in the cavern of “Vranduk-2” forecasted by the CFD-modelling, can be understood, up to the most important way, by the comparison of the simulated, developing fire-event of 40MW thermal-power, in it’s 25<sup>th</sup> and 119<sup>nd</sup> second, during which, this non-premixed combustion was going on, firstly without any ventilation in the tunnel. Employed *LES* turbulence-model was capable of demonstrating the fire shape and since we had

confinement of this motorway-tunnel in both of the cases of CFD-based exploring - the temperature zones were also easily recognizable. So, the expected negative impact, we saw in "Sentvid" northern tube - was displayed in the "Vranduk-2" as well, pointing to the fact that even in the 25<sup>th</sup> second (in case of scenario with non-ventilated tunnel cavern) the temperature level, for the RC-construction to decay, was unfortunately easily reached.

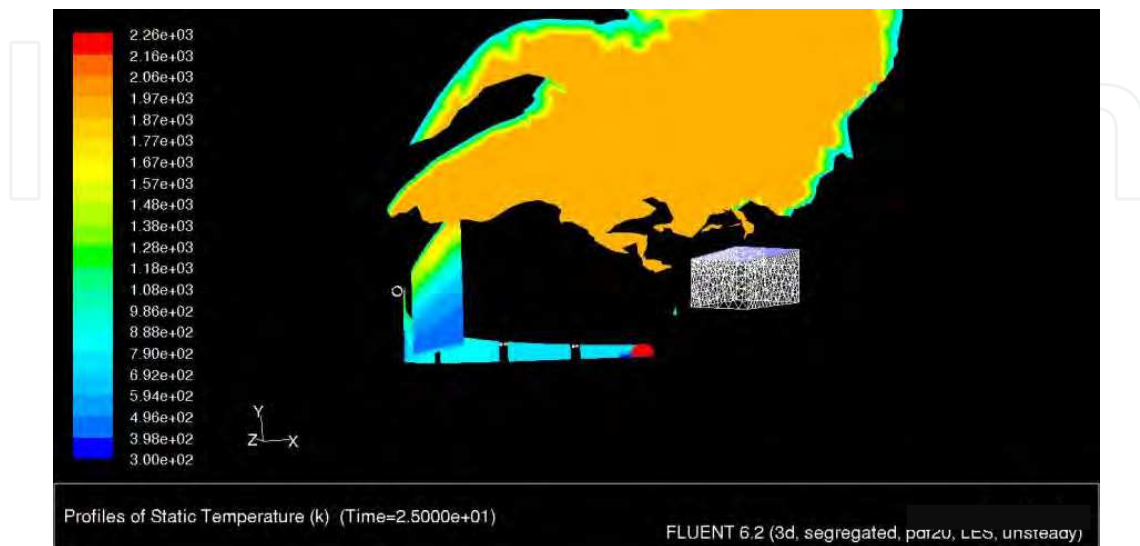


Fig. 5.2-1. In spite of the "dominance" of the iso-surface of 1800-K it is obvious that the thermal load of up to 40MW, that comes from accidental-fire in "Vranduk-2", will be negatively impacting the RC-construction (here: in the area of the fire-place, made visible by it's mesh, looking at the tunnel-ceiling "from below", we can see the eastern tunnel exit in far-part of the sketch)

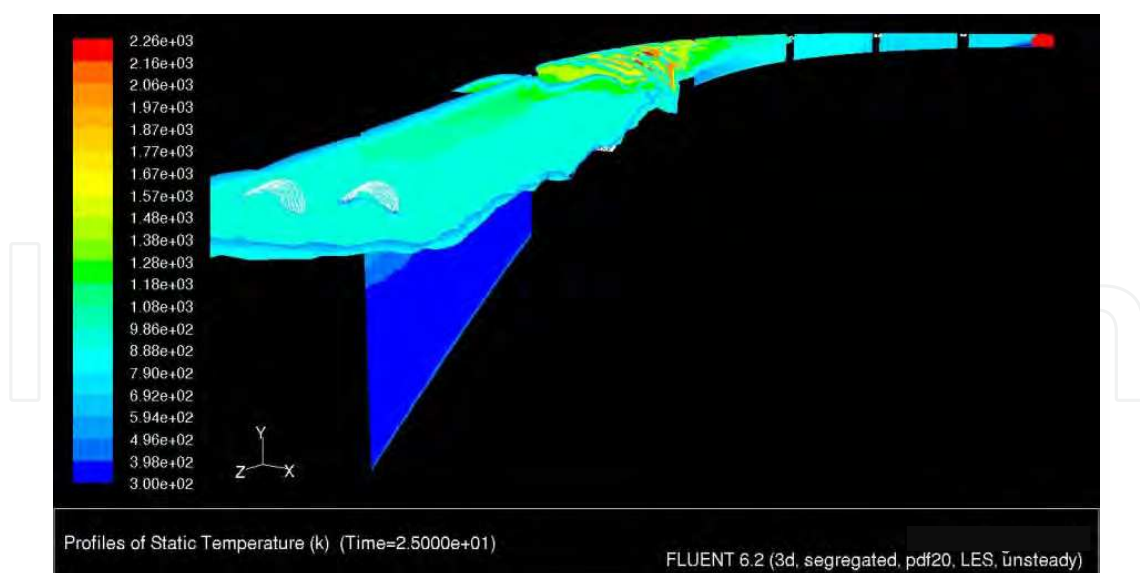


Fig. 5.2-2. The iso-surfaces of the performed temperatures due to the simulated large-scale non-premixed combustion do discover in first 25 seconds spreading of the negative thermal impact, along the "Vranduk-2" ceiling and the escorting tunnel body (the light blue-greenish temperature-area is a limit for a start of RC-decay due to the exposure to the accidental thermal load of 850 K). Far in this sketch one can notice the eastern-exit towards the city of Zenica. The canyon of the river Bosna is on the left-hand side

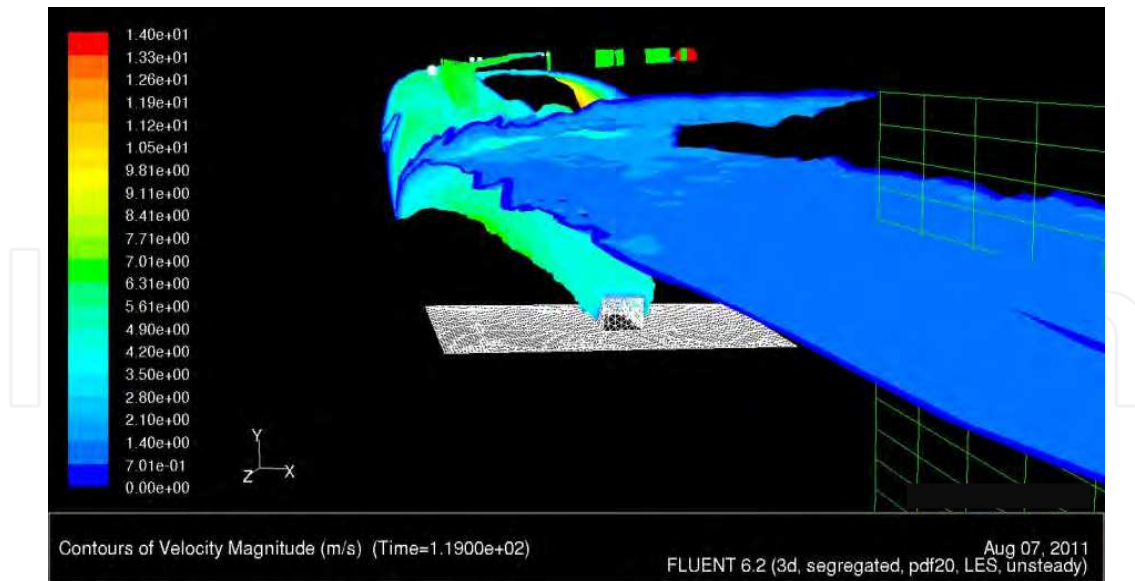


Fig. 5.2-3. The CFD-plotted iso-surface for the temperature of 600K is showing the velocities of the gaseous combustion products, as their spreading was forecasted throughout the cavern of “Vranduk-2”. In spite of natural draft towards the geodetically higher positioned eastern exit (far at the bottom of the sketch) in the 119<sup>th</sup> second, the employed LES-turbulence model forecasted also the back-layering towards the western cavern-exit.

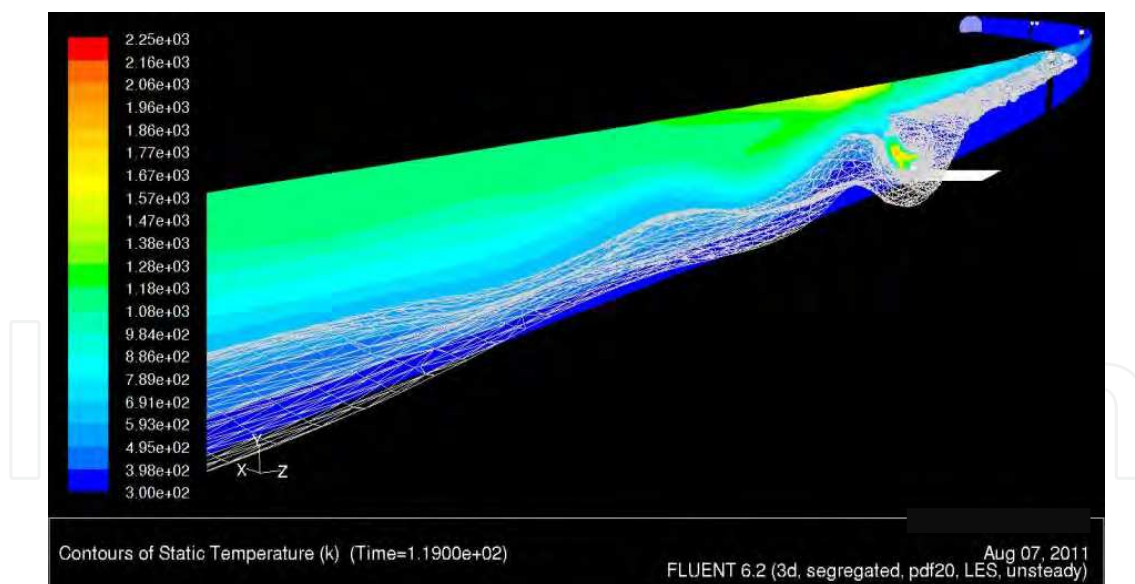


Fig. 5.2-4. The central control plane is intersecting the fire-place and pointing at the temperature zones. The displayed mesh is bordering the zone where thermal load can cause concrete destruction. Far down in the sketch one can see the western tunnel-entrance.

After 120s of modelling with CFD-tool on the scenario of a large-scale confined fire in “Vranduk-2” cavern – the artificial ventilation was employed. This forced air-flow was coming from the seven pairs of fans fixed to the ceiling along the tunnel-body, where each

of fourteen of them produced a longitudinal air-velocity of 39.1 m/s. As well as in case of "Sentvid" - also here is aim of such forced fluid-flow to envelope the existing non-premixed combustion (and it's consequences) and limit the possible damages to the RC-construction.

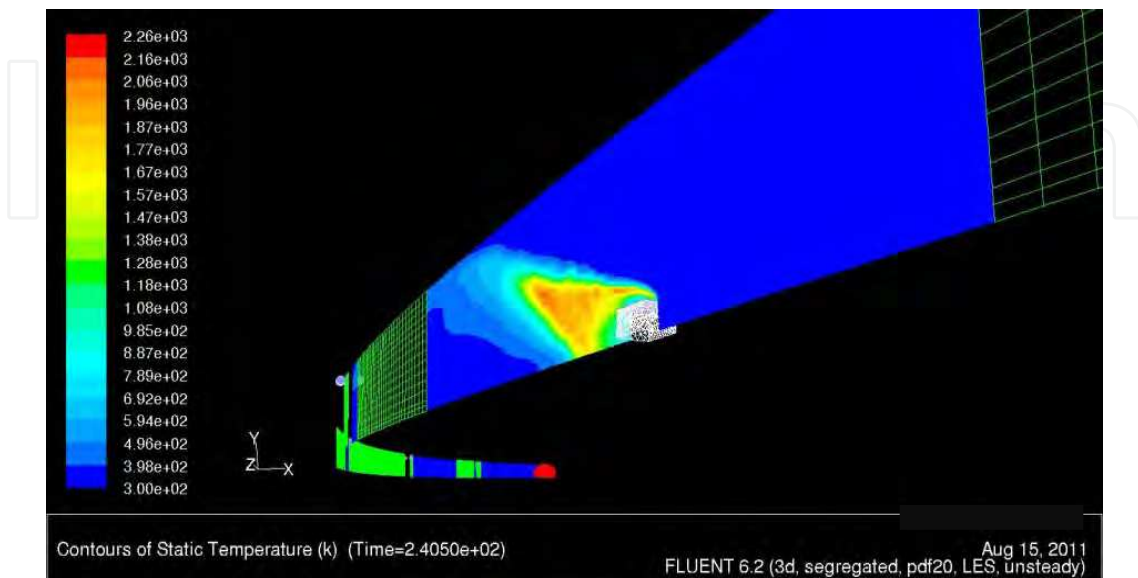


Fig. 5.2-5. The highest CFD-forecasted temperature is displayed already in the 25<sup>th</sup> second (modelled with employed LES-turbulence approach). Due to the energy transferring mechanism of convection, the heat is transmitted to the tunnel-ceiling and the iso-surfaces are pointing to the temperature decrease towards the tunnel body

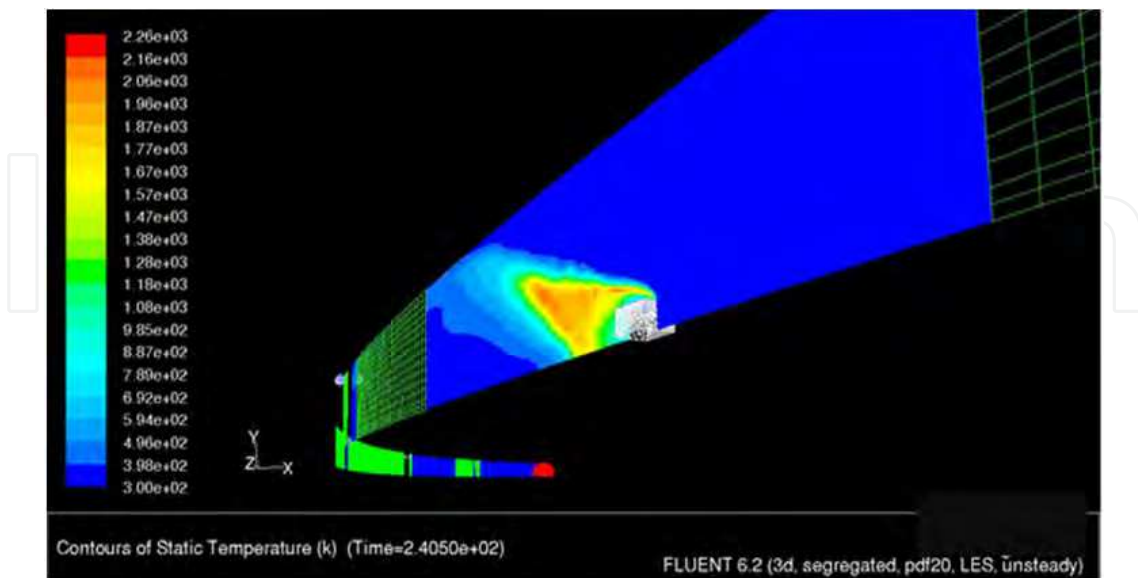


Fig. 5.2-6. In the 2<sup>nd</sup> minute of the employed ventilation (as simulated scenario was suggesting) the large scale fire and it's unwanted thermal load are suppressed

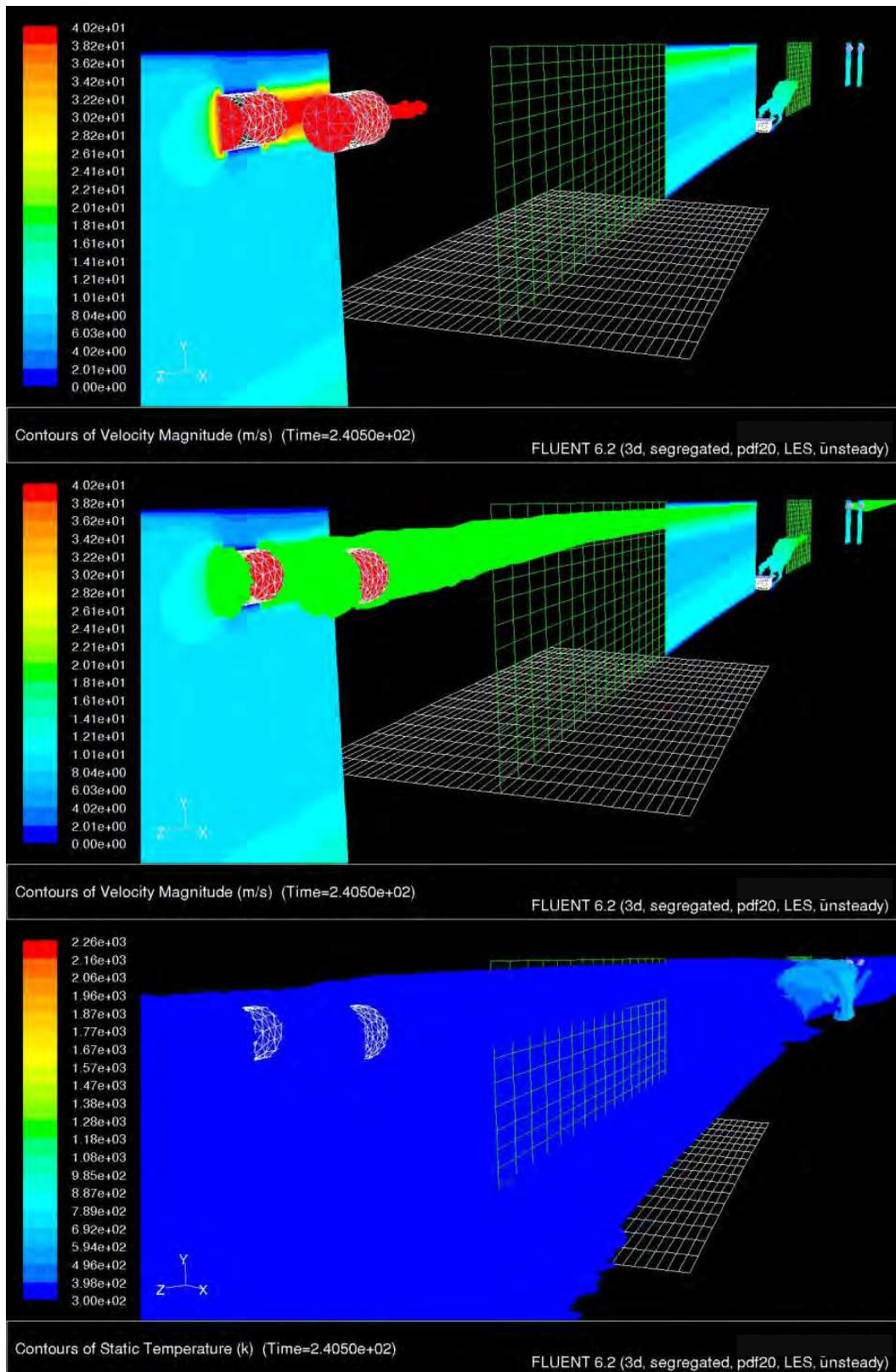


Fig. 5.2-7. The air-fans, looking towards the eastern exit of the “Vranduk-2” – And while the high temperature-zones of the fire were visible in first sketches, on the iso-surface for the 10m/s, the displayed temperature-zone is fully enveloping the near-fire-place. The accidental thermal load (deep in the sketch) is carried away by the forced air-flow

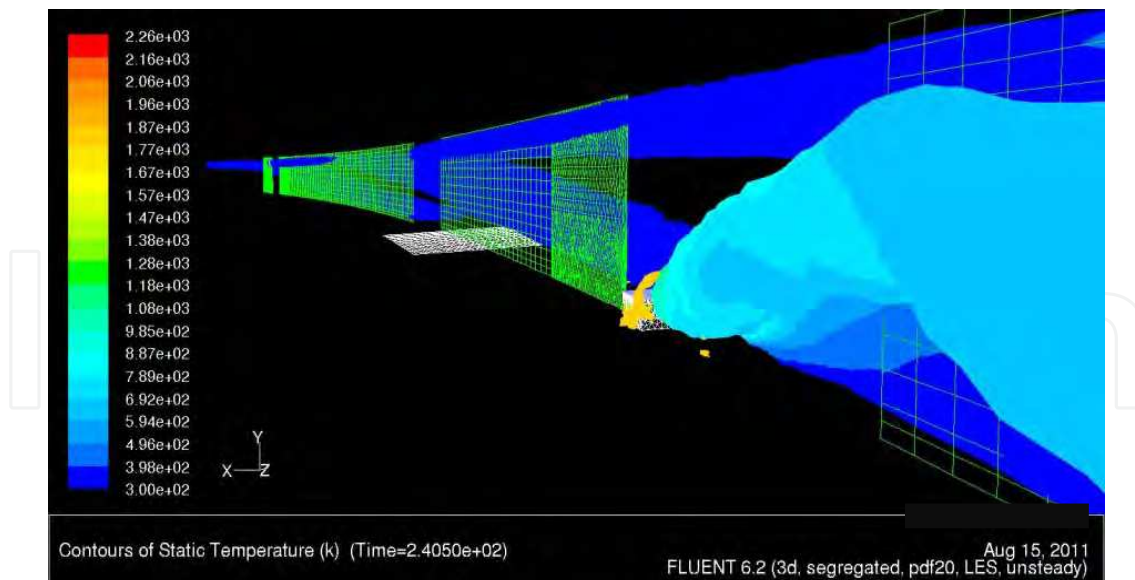


Fig. 5.2-8. Looking deeper into zones of the longitudinal ventilation – here the velocity of the forced air-flow of 13m/s is displaying the enveloping of the thermal influence in the 120<sup>th</sup> second of artificial air-flow. Looking towards the western entrance of “Vranduk-2” one can notice (deep down in the sketch) the velocity zones (blue) that are surrounding the air-fan pairs and “coming” towards the fire-place.

By performing this CFD-based study on covered traffic-objects of the given geometric characteristics within an existing road-infrastructure, the investigation on the accidental fire event was conducted according to the both planned scenarios of several experimental[33, 42, 44, 45] and computer aided[46-48] research[49, 50] research approaches. A “provocation” to conduct this research, was this specific geometry of the objects of interest, expecting new answers due to the possible impact of a reality-oriented traffic-enclosure (that was imbedded into a computational domain) onto this large-scale combustion and escorting occurrences. The CFD-demonstration in this attempt, pointed that the geometric characteristic of explored tunnels was not “strong enough” to give major influence to the propagation of the combustion consequences in the first 120s of non-ventilated space – as well as in the case of 120s-long ventilation time of the mentioned caverns. However in the near-fire place one was able to notice the asymmetric distribution of the gaseous products in “Vranduk-2” motorway-tunnel, over the tunnels’ ceiling and temperature’s iso-surfaces.

Giving the small mosaic-stone to the entire urge in the community; which is researching on large-scale confined fires, with the results of this research-attempt, it would be the intention of the presented study to address both the civil-engineering sector[51, 52] and enlarge database for the medical health-protection[53].

## 6. Acknowledgement

Medzid Muhasilovic thanks to Prof. Dr. Michel Deville for his unselfish on-going support as well as direct and indirect advices. Additional gratitude goes to Prof. Dr. Ivica Kozar for the ideas and both administrative and scientific support. In this sense, special thanks are made to Dr. Markus Gawlowski and to Dr. Iris Vela. Last but definitely not least, is that Medzid Muhasilovic specially thanks to Dipl.-Ing. Marko Zibert and Dipl.-Ing. Drago Dolenc.

## 7. References

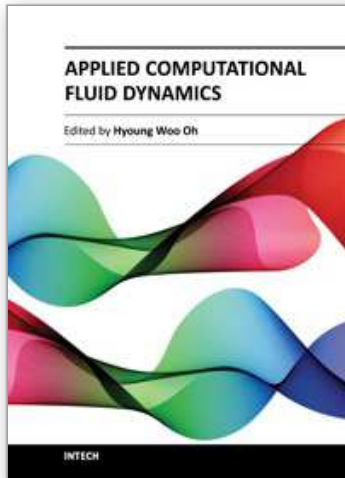
- [1] G. Holmstedt, S. Bengston, H. Tuovinen, Sensitivity Calculations of Tunnel fires Using CFD. *Fire Safety Journal*, 1996. 1: p. 99 - 119.
- [2] S. D. Miles, S. Kumar, R. D. Andrews. Validation of a CFD model for fires in the memorial tunnel. in *First International Conference on Tunnel Fires*. 1999. Lyon, France.
- [3] T. Heins, K. Kordina, Untersuchungen über die Brand- und Rauchentwicklung in Unterirdischen Verkehrsanlagen - Katastrophenschutz in Verkehrstunneln. 1990.
- [4] D. A. Charters, W. A. Gray, A. C. MacIntosh, A Computer Model to Assess Fire Hazards in Tunnels (FASIT). *Fire Technology*, 1994. 30: p. p. 143.
- [5] S. Kumar, G. Cox. Mathematical Modelling of Fires in Tunnels. in *5th International Symposium on the Aerodynamics & Ventilation of Vehicle Tunnels*. 1985.
- [6] S. Kumar, G. Cox. Radiation and Surface Roughness Effects in the Numerical Modelling of Enclosure Fires. in *Fire Safety Science - 2nd International Conference*. 1988.
- [7] Chasse, P. Sensitivity Study of Different Modelling Techniques for the Computer Simulation of Tunnel Fire: Comparison with Experimental Measures. in *First CFDS International User Conference*. 1993. Oxford, UK.
- [8] H. Briollay, P. Chasse, Validating and Optimizing 2D and 3D Computer Simulations for the Offenegg Tunnel Fire Test. 1994, Centre d'Etudes des Tunnels: Bron Cedex.
- [9] S. Kumar, G. Cox, Mathematical Modelling of Fires in Tunnels - Validation of JASMINE. 1986, Transport and Research Laboratory Contractor: Crowthorn, UK.
- [10] Tuovinen, H., Validation of Ceiling Jet Flows in a Large Corridor with Vents Using the CFD Code JASMINE. *Fire Technology*, 1994. 32.
- [11] Kunsch, J. P., Simple model for control of fire gases in a ventilated tunnel. *Fire Safety Journal*, 2002. 37: p. 67-81.
- [12] A. Beard, D. Drysdale, P. Holborn, S. Bishop, Configuration Factor for Radiation in a Tunnel or Partial Cylinder. *Fire Technology*, 1993. 29.
- [13] Miles, S. D., About JASMINE, D.M. Muhasilovic, Editor. 2006: Edinburgh, Essen.
- [14] B. F. Magnussen, B. H. Hjertager. On mathematical modelling of turbulent combustion with special emphasis on soot formation and combustion. in *16th international symposium on combustion*. 1976. Pittsburgh, USA.
- [15] S. D. Miles, S. Kumar. Computer modelling to assess the benefits of road tunnel fire safety measures. in *Inflam 2004*. 2004. Edinburgh, Scotland, UK.
- [16] K. B. McGrattan, A. Hamins, Numerical Simulation of the Howard Street Tunnel Fire. 2002, NIST: Gaithersburg, USA.
- [17] <http://www.tunnelfire.com>.
- [18] Wehlan, M., On "Memorial Tunnel Experiments" (personal communication). 2006: Washington(USA), Podgora(Croatia).
- [19] M. K.-A. Neophytou, R. E. Britter, A simple model for the movement of fire smoke in a confined tunnel. *Pure and Applied Geophysics*, 2005. 162: p. 1941.
- [20] P. Z. Gao, S. L. Liu, W. K. Chow, N. K. Fong, Large eddy simulations for studying tunnel smoke ventilation. *Tunneling and Underground Space Technology*, 2004. 19: p. 577.
- [21] M. Peric, J. H. Ferziger, *Computational Methods for Fluid Mechanics*. 2001, Berlin: Springer Verlag. 423.

- [22] H. R. Baum, et. al. Gravity-current transport in buildings fires. in International Conference on Fire Research and Engineering. 1995. Orlando, Florida, USA.
- [23] Vladimirova, N., Model flames in the Boussinesq limit. 2006, ASC / Flash Center, Dept. of Astronomy and Astrophysics, The University of Chicago, IL 60637: Chicago, USA.
- [24] T. B. Gatski, T. Jongen, Nonlinear eddy viscosity and algebraic stress models for solving complex turbulent flows. *Progress in Aerospace Sciences*, 2000. 36: p. 655.
- [25] Leupi, C., Numerical modeling of cohesive sediment transport and bed morphology in estuaries, in La faculte sciences at techniques de l'ingenieur. 2005, Ecole Polytechnique Federale de Lausanne: Lausanne.
- [26] W. Zhang, et. al., Turbulence statistics in a fire room model by large eddy simulation. *Fire Safety Journal*, 2002. 37: p. 721.
- [27] <http://www.fluent.com>.
- [28] P. J. Woodburn, R. E. Britter, CFD-simulations of a tunnel fire - part one. *Fire Safety Journal*, 1996. 26: p. 35.
- [29] N. C. Markatos, M. R. Malin, Mathematical modelling of buoyancy-induced smoke flow in enclosures. *International Journal of Heat Mass Transfer*, 1982. 25: p. 63.
- [30] S. M. Jojo, W. K. Chow, Numerical studies on performance evaluation of tunnel ventilation safety systems. *Tunneling and Underground Space Technology*, 2003. 18: p. 435.
- [31] C. K. Westbrook, W. J. Pitz, H. J. Curran, Chemical kinetic modelling study of the effects of Oxygenated hydrocarbons on soot emissions from diesel engines. *Journal of Physical Chemistry*, 2006. 110: p. 6912.
- [32] O. Megret, O. Vauquelin, A model to evaluate tunnel fire characteristics. *Fire Safety Journal*, 2000. 34: p. 393.
- [33] H. K. Versteeg, W. Malalasekera, *An Introduction to computational fluid dynamics*. 1995, London: Longman Group Ltd.
- [34] Hirsch, C., *Numerical Computation of Internal and External Flows*. Vol. I. 1988, Chichester Brisbane Toronto New York: John Wiley & Sons. 515.
- [35] <http://lin.epfl.ch>.
- [36] Muhasilovic, M., CFD-approach in investigation of consequences of accidental large-scale fires in road tunnels with natural ventilation, in STI-ISE-LIN. 2007, EPFL: Lausanne, Switzerland.
- [37] Babrauskas, V., Estimating large pool fire burning rates. *Fire Technology*, 1983. 19: p. 251.
- [38] I. Vela, et. al. Scale Adaptive Simulation (SAS) of heat radiation and soot amount in a large-scale turbulent JP-4 pool fire. in DECHEMA Tagung. 2006. Wiesbaden, Germany.
- [39] <http://lmr.epfl.ch>.
- [40] <http://www.also-natursteine.de>.
- [41] H. Koseki, T. Yumoto, Air entrainment and thermal radiation from heptane pool-fires. *Fire Technology*, 1988. 24: p. 33.
- [42] H. Kurioka, Y. Oka, H. Satoh, O. Sugawa, Fire Properties in Near Field of Square Fire Source with Longitudinal Ventilation in Tunnels. *Fire Safety Journal*, 2003. 34(4): p. 319 - 340.
- [43] Modic, J., Fire Simulation in Road Tunnels. *Tunneling and Underground Space Technology*, 2003. 18: p. 525 - 530.



- [44] H. Kurioka, Y. Oka, H. Satoh, H. Kuwana, O. Sugawa, Properties of the Plume and Near Fire Source in horizontally long and narrow spaces. *Journal of Construction Engineering*, 2001(546): p. 151 - 156.
- [45] O. Vauquelin, O. Megret, Smoke extraction experiments in case of fire in a tunnel. *Fire Safety Journal*, 2002. 37: p. 525.
- [46] Ingason, H., Correlation between temperatures and oxygen measurements in a tunnel flow. *Fire Safety Journal*, 2007. 42: p. 75.
- [47] O. Vauquelin, Y. Wu, Influence of tunnel width on longitudinal smoke control. *Fire Safety Journal*, 2006. 41: p. 420.
- [48] P. J. Woodburn, R. E. Britter, CFD Simulation of a Tunnel Fire - part two. *Fire Safety Journal*, 1996. 26: p. 63.
- [49] G. B. Grant, S. F. Jagger, C. J. Lea, Fires in Tunnels. *Philosophical Transactions: Methematical, Physical, Engineering Sciences*, 1998: p. 2873.
- [50] S. R. Lee, H. S. Ryou, A numerical study on smoke movement in longitudinal ventilation tunnel fires for different aspect ratio. *Building and Environment*, 2006. 41: p. 719.
- [51] R. O. Carvel, A. N. Beard, P. W. Jowitt, The influence of longitudinal ventilation systems on fires in tunnels. *Tunneling and Underground Space Technology*, 2001. 16: p. 3.
- [52] V. K. R. Kodur, L. A. Bisby, M. F. Green, Experimental evaluation of the fire behaviour of insulated fibre-reinforced-polymer-strengthened reinforced concrete columns. *Fire Safety Journal*, 2006. 41: p. 547.
- [53] F. Wald, et. al., Experimental behaviour of a steel structure under natural fire. *Fire Safety Journal*, 2006. 41: p. 509.
- [54] F. Lestari, et. al., An alternative method for fire smoke toxicity assessment using human lung cells. *Fire Safety Journal*, 2006. 41: p. 605.

IntechOpen



## **Applied Computational Fluid Dynamics**

Edited by Prof. Hyoung Woo Oh

ISBN 978-953-51-0271-7

Hard cover, 344 pages

**Publisher** InTech

**Published online** 14, March, 2012

**Published in print edition** March, 2012

This book is served as a reference text to meet the needs of advanced scientists and research engineers who seek for their own computational fluid dynamics (CFD) skills to solve a variety of fluid flow problems. Key Features: - Flow Modeling in Sedimentation Tank, - Greenhouse Environment, - Hypersonic Aerodynamics, - Cooling Systems Design, - Photochemical Reaction Engineering, - Atmospheric Reentry Problem, - Fluid-Structure Interaction (FSI), - Atomization, - Hydraulic Component Design, - Air Conditioning System, - Industrial Applications of CFD

### **How to reference**

In order to correctly reference this scholarly work, feel free to copy and paste the following:

M. Muhasilovic, A. Mededovic, E. Gacanin, K. Ciahotny and V. Koza (2012). Air Movement Within Enclosed Road-Objects with Contra-Traffic CFD-Investigation, Applied Computational Fluid Dynamics, Prof. Hyoung Woo Oh (Ed.), ISBN: 978-953-51-0271-7, InTech, Available from: <http://www.intechopen.com/books/applied-computational-fluid-dynamics/air-movement-within-enclosed-road-objects-with-contra-traffic-a-cfd-investigation>

# **INTECH**

open science | open minds

### **InTech Europe**

University Campus STeP Ri  
Slavka Krautzeka 83/A  
51000 Rijeka, Croatia  
Phone: +385 (51) 770 447  
Fax: +385 (51) 686 166  
[www.intechopen.com](http://www.intechopen.com)

### **InTech China**

Unit 405, Office Block, Hotel Equatorial Shanghai  
No.65, Yan An Road (West), Shanghai, 200040, China  
中国上海市延安西路65号上海国际贵都大饭店办公楼405单元  
Phone: +86-21-62489820  
Fax: +86-21-62489821

© 2012 The Author(s). Licensee IntechOpen. This is an open access article distributed under the terms of the [Creative Commons Attribution 3.0 License](#), which permits unrestricted use, distribution, and reproduction in any medium, provided the original work is properly cited.

IntechOpen

IntechOpen